Received: 6 August 2021 | Revised: 28 August 2021 | Accepted: 5 September 2021

DOI: 10.1002/jcu.23068

WILEY

RESEARCH ARTICLE

Seeing the unseen with superb microvascular imaging: Ultrasound depiction of normal dermis vessels

Antonio Corvino MD, PhD[1] | Carlo Varelli MD[2] | Giulio Cocco MD[3] | Fabio Corvino MD[4] | Orlando Catalano MD[2]

[1]Motor Science and Wellness Department, University of Naples "Parthenope", Naples, Italy

[2]Radiology Unit, Istituto Diagnostico Varelli, Naples, Italy

[3]Unit of Ultrasound in Internal Medicine, Department of Medicine and Aging Sciences, University of Chieti G d'Annunzio, Chieti, Italy

[4]Vascular and Interventional Radiology Department, Cardarelli Hospital, Naples, Italy

Correspondence
Antonio Corvino, MD, PhD, Motor Science and Wellness Department, University of Naples "Parthenope", via F. Acton 38, Naples I-80133, Italy.
Email: an.cor@hotmail.it

Abstract

Purpose: Current color- and power-Doppler techniques cannot demonstrate vascularization of the dermis. Aim of this prospective study was to investigate whether the new superb vascular imaging (SMI) technique improves the ultrasound (US) depiction of dermis vessels in healthy volunteers. SMI was compared side-by-side to conventional power-Doppler (PD) imaging.

Methods: Thirty adult subjects (18 men and 12 women, mean age 45 years old) were evaluated with US at level of five body areas: forehead, forearm, palm, buttock, and thigh. The vascular index (VI) was employed to objectively quantify the difference between SMI and PD imaging in terms of dermis flow amount.

Results: Forehead VI was higher for SMI than for PD in 93% of cases, forearm VI was higher for SMI than for PD in 97% of cases, palm VI was higher for SMI than for PD in 87% of cases, buttock VI was higher for SMI than for PD in 100% of cases, thigh VI was higher for SMI than for PD in 100% of cases. SMI-detected vascular signals in 100% of the body areas. PD failed to show any flow signals from the forehead in 23% of cases, forearm in 37% of cases, palm in 33% of cases, buttock in 47% of cases, and thigh in 50% of cases.

Conclusion: SMI can demonstrate normal dermis vascularization whereas conventional PD cannot. SMI is a sensitive and promising technique in the study of dermis abnormalities, particularly when quantifying the disease activity is important.

KEYWORDS
dermal vessels, dermatology ultrasound, Doppler ultrasound (US), power-Doppler (PD), superb microvascular imaging (SMI)

1 | INTRODUCTION

The skin is composed by the epidermis and the dermis, the latter consisting for 70% of connective tissue.[1–3] Dermis thickness varies in the different body areas, decreasing with aging.[1–4] The dermis has an intense vascularization, particularly in its deeper aspect.[1–3] This vascular network serves a number of vital functions such as nutritional support for tissues and homeostasis.[5] However, dermis vessels are usually not

Abbreviations: PD, power Doppler; SMI, superb microvascular imaging; US, ultrasound; VI, vascular index.

We confirm that this work is original and has not been published elsewhere nor is it currently under consideration for publication elsewhere.

detectable in healthy subjects using color-Doppler and power-Doppler (PD) imaging.[3,5–8] This limitation is due to the small size of the vessels and to their slow velocity, commonly equal to or less than 2 cm/s. In the last years, several companies have developed advanced technologies for the ultrasound (US) study of the microvasculature. We hypothesized that these new techniques may allow detecting some more flow signals in the dermis compared to conventional PD imaging. Consequently, we prospectively compared PD and superb microvascular imaging (SMI, Canon Medical Systems, Tokyo, Japan) in the assessment of dermal vessels in healthy subjects (Figure 1).

2 | MATERIALS AND METHODS

2.1 | Study design and subjects

The study was developed as a single-center, prospective experience on healthy adult volunteers. The study protocol was reviewed and approved by our institutional review board and was conducted according to Good Clinical Practice and the Declaration of Helsinki. All participants provided written informed consent. The skin of the selected anatomical areas was inspected and subjects with cutaneous abnormalities were excluded. Hence, inclusion criteria were age above 18 years old and absence of any skin abnormality at both physical inspection and ultrasound exploration.

Thirty Caucasian subjects were enrolled between September 2020 and December 2020. There were 18 males and 12 females, aged 20–77 years (mean, 45 years old).

2.2 | Ultrasound technique

Two radiologists with respectively 23 and 12 years of experience with US acquired each one the images of 15 random subjects. Care was taken to avoid an excessively low temperature in the room. We choose to study the following five body areas: forehead, dorsal aspect of the forearm, hand palm, buttock, and anterior aspect of the thigh. These anatomical sites were chosen considering some published articles on US assessment of skin thickness skin and echogenicity in sun-exposed and non-sun exposed areas as well as to study both glabrous and non-glabrous skin.[2,9–11]

Gray-scale US, SMI, and PD images were obtained on an Aplio i800 system (Canon Medical Systems Corporation) equipped with a 22-MHz hockey stick-shaped linear array transducer. First a good quality skin image was taken on the gray-scale, using a large amount of ultrasound gel. SMI was then performed, in the color mode, with the following parameters: velocity scale, 1.5 cm/s; frame rate, 57 frames per second; filter 4 (range, 0–7); and dynamic range, 75 dB. The systolic cardiac phase in which the vascular codes were brightest and largest was caught in all cine images to exclude differences caused by pulsatility.[12] In each body area, the flow signals were first searched by using SMI. Then, once that a clear SMI scan showing dermis vessels was taken, this image was freeze on the split-screen and then a corresponding PD scan was quickly obtained. The operator froze the PD acquisition and went back to the frame showing the largest amount of flow signal, storing it in the scanner archive. PD parameters were as follows: monochromatic code, velocity scale, 2.8 cm/s; frame rate, 19 frames per second; filter 2 (range, 0–7), and dynamic range, 75 dB. For both SMI and PD imaging care was taken to avoid motion of the operator's hand or the transducer, which

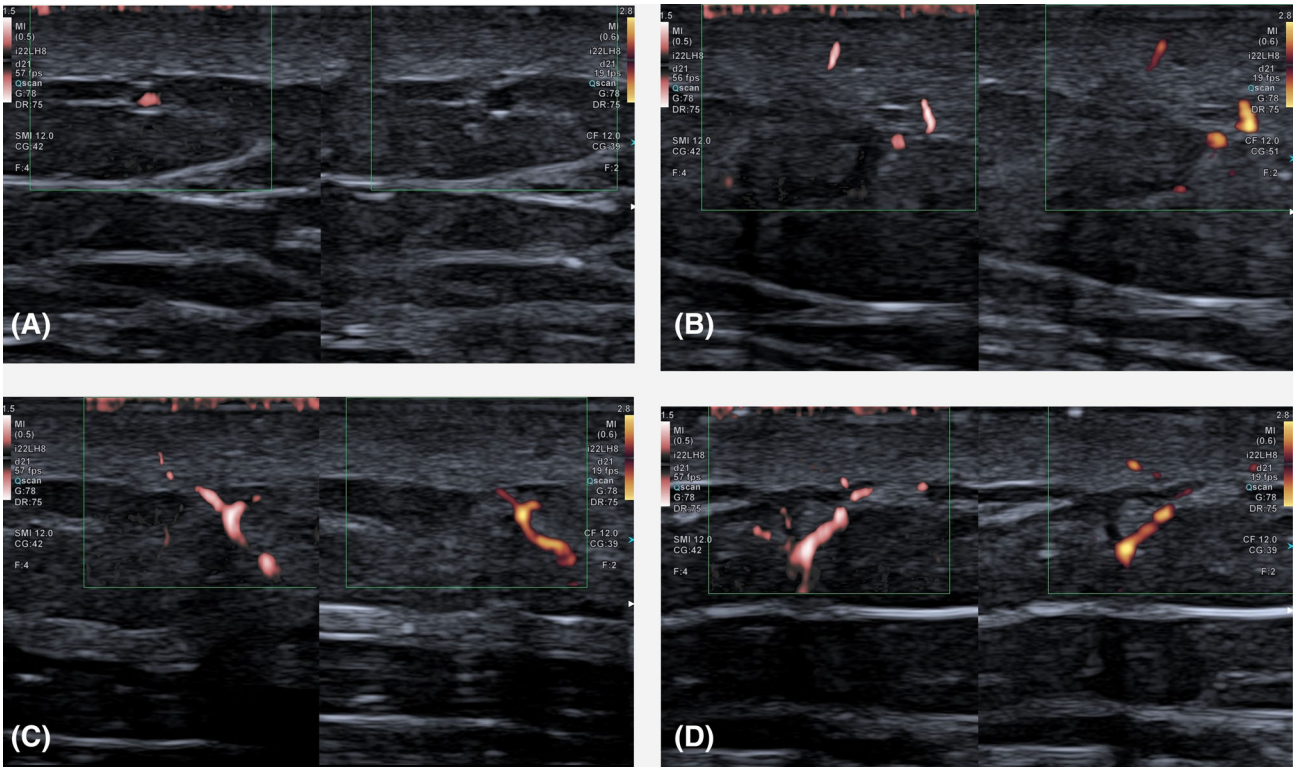

FIGURE 1 Subjective scoring of the flow signals amount in the dermis. No flows at SMI and PD (a), comparable flows at SMI and at PD (b), more flows at SMI than at PD (c), more flows at PD than at SMI (d). Flow signals in the subcutaneous layer were not considered in this study

TABLE 1 Number of color pixels at SMI and at PD in 30 subjects at level of five different anatomic areas

		Body areas									
		Forehead		Forearm		Palm		Buttock		Thigh	
Subjects	Sex/age	SMI pixels	PD pixels	SMI pixels	PD pixels	SMI pixels	PD pixels	SMI pixels	PD pixels	SMI pixels	PD pixels
1	M/33	745	819	433	0	4548	3227	4543	78	344	0
2	M/41	1829	78	493	19	3289	2349	79	0	2309	0
3	F/67	602	0	6523	5898	813	28	327	0	934	412
4	M/20	6539	2301	2319	0	2232	3989	1227	0	369	0
5	F/40	872	129	1126	0	7645	7005	9132	2302	517	0
6	M/55	4502	3611	5237	4234	38	0	4209	0	5643	673
7	M/77	1002	321	7614	5493	812	802	3427	0	5638	788
8	F/55	529	0	5334	0	2347	57	348	47	588	0
9	M/60	921	622	3209	934	1021	0	6543	332	8208	990
10	F/42	848	340	1321	768	1876	0	5732	0	805	0
11	M/21	831	527	610	99	1860	1060	4390	90	452	27
12	M/21	3006	2143	562	0	1211	2356	4219	0	708	345
13	M/29	4775	807	1079	0	3443	271	3343	3245	4427	0
14	F/33	328	0	5742	4392	299	0	5837	3228	4376	564
15	M/65	788	622	4215	2311	4468	2511	459	0	6732	0
16	F/57	333	321	5659	0	2418	0	1446	0	663	0
17	M/43	476	428	4311	3218	7412	427	7432	329	389	276
18	F/57	481	519	1933	0	3437	276	3225	553	6866	222
19	M/38	336	291	6765	3423	374	0	4337	0	6534	0
20	F/28	1221	0	933	1206	3254	3345	332	111	1723	0
21	M/66	5904	3320	3321	234	1822	1731	568	0	6578	430
22	M/43	868	29	234	211	2476	0	6745	0	7262	1656
23	F/34	457	16	2320	0	2365	177	5698	0	2376	0
24	M/32	589	0	3278	1202	288	32	511	342	3423	0
25	F/47	9929	1302	5632	467	2654	211	2222	69	3766	324
26	M/76	4343	399	3328	0	6452	29	6598	0	3654	267
27	F/51	731	0	8345	3211	92	0	7056	4222	769	86
28	M/45	3320	2786	3377	342	9222	0	5678	2367	858	0
29	M/47	4211	0	326	0	478	976	3889	455	7623	6321
30	F/40	2478	1325	877	23	374	0	459	215	1234	0
		Mean, 2047	Mean, 769	Mean, 3215	Mean, 1256	Mean, 3118	Mean, 1029	Mean, 3667	Mean, 600	Mean, 3192	Mean, 436

Abbreviations: F, female; M, male; PD, power-Doppler; SMI, superb microvascular imaging.

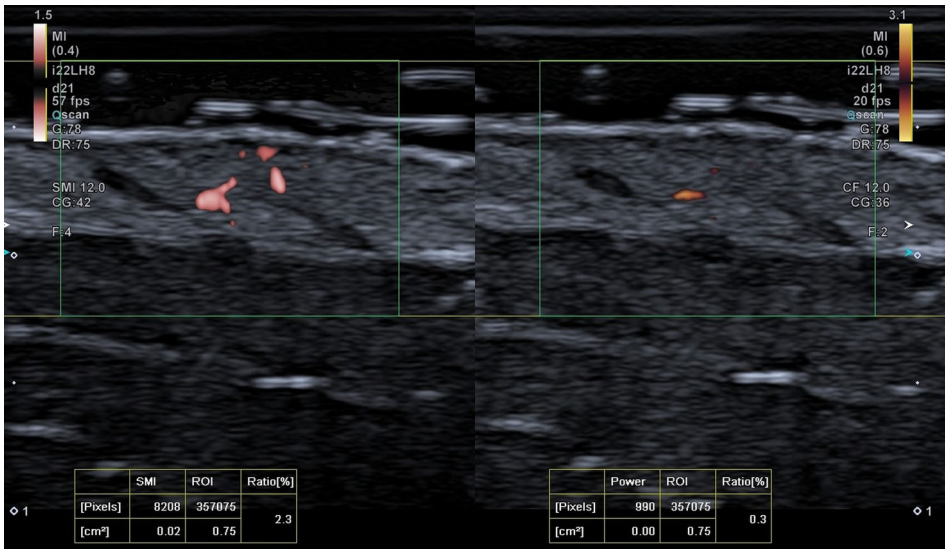

FIGURE 2 Sixty-year-old asymptomatic male. Dermis vascularization in the thigh at SMI (left part of the image), with 8208 colored pixels, and at PD (right part of the image), with 990 colored pixels

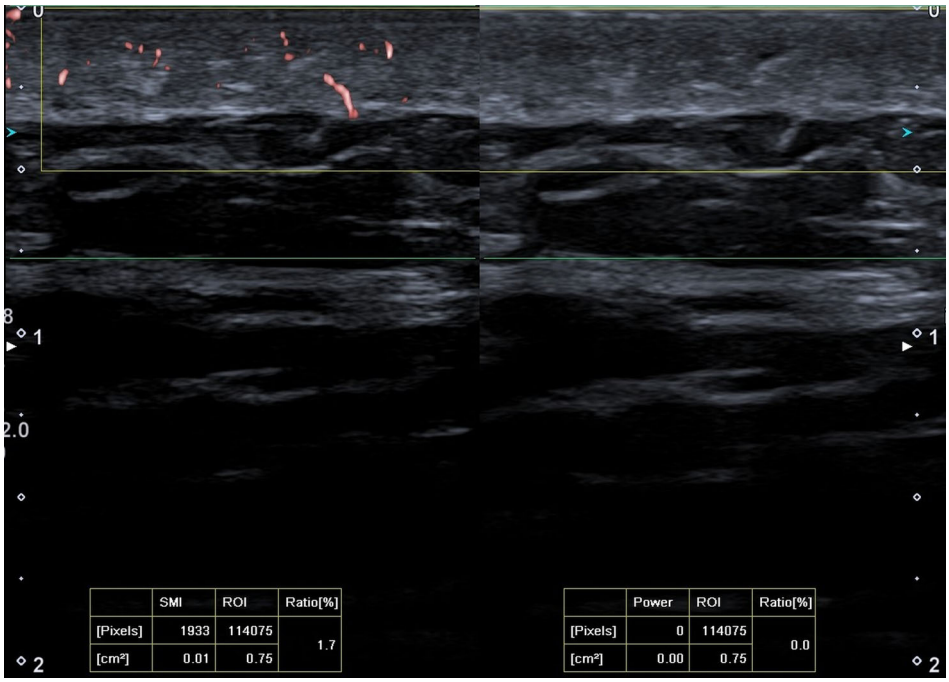

FIGURE 3 Fifty-seven-year-old asymptomatic female. Dermis vascularization in the forearm at SMI (left part of the image), with 1933 colored pixels, and at PD (right part of the image), with 0 colored pixels

was placed gently above the gel layer. The beam focus was placed at the dermis-hypodermis edge both for SMI and PD imaging. The color gain was not changed between the two techniques.

2.3 | Images analysis

To obtain an objective, quantitative assessment of flow signals in PD imaging and in SMI we employed the vascularity index (VI), which determines the number and percentage of color pixels in the total gray-scale pixels in a defined region of interest (ROI).[12–14] Starting from the saved double-screen image containing the SMI scan on the left and the PD scan on the right, we placed an identical rectangular ROI on both images to assess the VI. Care was taken to exclude the subcutaneous vessels and to include in the ROI only signals from the dermis. The color artifacts, defined as random and transient colored pixels not representing true flows, were always excluded from the ROI. These noise artifacts were sometimes present in the images, particularly on the SMI scans and, especially at the uppermost portion of the field of view, but care was used to review the frames and choose clear scans without any motion color artifact. The number of pixels with flow signals was recorded for both SMI and PD imaging for each anatomical site.

2.4 | Statistical analysis

All of the statistical analyses were performed with MedCalc for Microsoft Windows (version 13.1.2.0, MedCalc). For comparison of

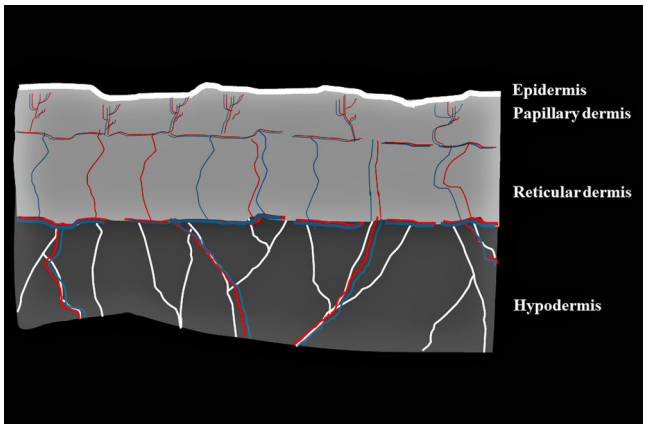

FIGURE 4 Drawing showing schematically the normal skin vascularization. Large, subcutaneous vessels reach the dermis and form a superficial and a deep horizontal plexus

the sensitivity between the SMI and PD in detection of flow signals for each anatomical site, the McNemar test was applied. A two-tailed *P* value of less than 0.05 was considered to indicate a statistically significant difference.

3 | RESULTS

The mean number of colored pixels was 2047 for SMI and 769 for PD at level of the forehead, 3215 for SMI and 1256 for PD at level of the forearm, 3118 for SMI and 1029 for PD at level of the palm, 3667 for SMI and 600 for PD at level of the buttock, and 3192 for SMI and 436 for PD at level of the thigh (Table 1). Overall, mean VI was higher for SMI than for PD for all 30 subjects (100%). Regarding each anatomic area, forehead VI was higher for SMI than for PD in 28 out of 30 cases (93%), forearm VI was higher for SMI than for PD in 29 out of 30 cases (97%), palm VI was higher for SMI than for PD in 26 out of 30 cases (87%), buttock VI was higher for SMI than for PD in 30 out of 30 cases (100%), thigh VI was higher for SMI than for PD in 30 out of 30 cases (100%; Figure 2).

SMI, by detecting vascular signals in all 180 body areas, showed a sensitivity value much higher than PD (100% vs. 86%). PD even failed to show any flow signals in 7 out of 30 cases in the forehead (23%), 11 of 30 cases in the forearm (37%), 10 of 30 cases in the palm (33%), 14 of 30 cases in the buttock (47%), and 15 of 30 cases in the thigh (50%; Figure 3). The difference in terms of sensitivity was statistically significant for all the body areas investigated. The *P* value was less than 0.0001 for the forehead, forearm, and palm. It equaled 0.0002 for the buttock and 0.0003 for the thigh.

4 | DISCUSSION

The dermis has a mesodermal origin and is dominated by packages of organized collagen, providing the supporting structure to the skin.[15] On US it appears as a moderately echoic layer just below the thin, more hyperechoic epidermis.[3,6] From the histological point of view, the dermis includes the thinner, superficial layer of the papillary dermis, and the thicker and more profound layer of the reticular dermis. These two layers differ in the way collagen fibers are arranged, being denser in the reticular dermis.[1,8] US cannot readily differentiate these two portions, although the papillary dermis may be less echoic than the reticular one. The dermis includes blood vessels, lymphatics, nerves, hair follicles, and sweat glands.[1,16] Dermis vascularization decreases with aging, with a lower vascular density and a smaller vessels diameter in the elder than in the young.[7,17,18] The structure of vessels is arranged into superficial and deep horizontal plexuses (Figure 4).[5] A deep plexus, made by relatively larger vessels, mostly veins, is located at the interface of the dermis and subcutis. It is fed by branches of the large subcutaneous arteries. Vessels caliber in the reticular dermis, ranges from 50 to 150 μm.[19] The border between papillary and reticular dermis hosts a superficial plexus that supplies the dermal papillae through a candelabra-like capillary system.[8,20] This superficial plexus is located 1–1.5 mm below the skin surface and consists of vessels less than 50 μm in caliber. The two horizontal plexuses are connected by direct, vertical, arborizing channels.[19]

In the US assessment of vascularization of breast and thyroid nodules, for example, the difficulty resides in the small caliber of the vessels and in the slow flow of the blood inside them. For the skin assessment, there are two additional obstacles. The first one is the pressure applied by the transducer, even if the operator hold the probe gently. The second difficulty is the closeness of the skin vessels to the transducer footprint. It is known that the field-of-view area close to the transducer, called the Fresnel zone or near field, is the one better seen at ultrasound since the beam is collimated and the resolution is high. Instead, at some point distal to the transducer, in the far-field or Fraunhofer zone, the beam begins to diverge with decreased resolution. However, the region nearest to the probe is compressed in ultrasound image, for a length that depends on the transducer quality and on the emission frequency.[21–23]

Several strategies have been proposed to improve the ultrasound display of superficial, slow flows at color- and PD imaging. These include optimization of scanning setting sensitivity (small color box, high transmission frequency, low pulse repetition frequency, low or null wall filter, high color gain),[6,24] interposition of gel stand-off pads,[21] use ultra-high frequencies,[25] injection of microbubbles.[26] Due to the intrinsic limitations of Doppler techniques, however, none of these options allows an adequate assessment of normal dermis vessels.

SMI applies clutter suppression algorithm that separates flow signals from overlying tissue motion artifacts. Consequently, SMI allows preserving the low-flow components, which are removed by conventional wall filters in color- and PD imaging, while displaying flow signals with a high spatial resolution and high frame rates.[27] SMI uses higher frame rates than PD, more than 50 Hz, and lower pulse repetition frequencies ranging between 220 and 234 Hz.[12] It analyzes the characteristics of motion artifacts arising from nearby structures and extracts the relevant information.[28] SMI has proven effective in detecting small vessels in cases where color- and power-Doppler failed to identify any flow signal.[27,29] By now, this technique has been

tested in a number of superficial and abdominal anatomical sites.[13,14,27–29] Govind and coworkers found that SMI is more sensitive than color Doppler in demonstrating microvenous reflux in limbs with venous disease and SMI.[30] İslamoğlu and Uysal employed SMI to assess plaques of cicatricial alopecia.[31] To our knowledge, no study has investigated yet the value of SMI in studying skin vascularization. Dermatology is a growing field of application of ultrasound.[4,7,24,32] The availability of a technique capable to demonstrate dermal flows can be useful in evaluating the activity status of a number of skin abnormalities, including morphea, psoriasis, cutaneous vasculitides, suppurative hidradenitis, burns, wounds, and surgical flaps.[4,19,33,34] Our study proved that SMI is by far more sensitive than PD in detecting dermal flows. The difference is probably even higher than what found in our study. In SMI, the color signal is visible only in the vessels while in PD color typically bleeds out of the lumen. This blooming partially compensated at VI assessment the poor sensitivity of PD. Despite this, SMI was significantly more sensitive than PD.

There are some limitations to our study. Firstly, it was conducted in a single center, and the number of cases was relatively small. Secondly, the choice of the anatomical sites to be sampled was somehow arbitrary. However, since the difference between SMI and PD imaging performance was so marked, it is our opinion that similar results would have been obtained also if scanning other anatomical locations. Thirdly, although care was taken to obtain adequately matching scans between SMI and PD, these scans could not be perfectly identical each other. Finally, we made no attempt to differentiate dermis vessels into arteries and veins. This aspect was not relevant for the study purpose and, additionally, the vessels we investigated were too small to obtain an adequate spectral sampling.

In conclusion, new microvascular imaging techniques such as SMI allow reliable ultrasound display of normal dermis flows while conventional PD imaging cannot. This opens new perspectives in the assessment of dermal abnormalities.

ACKNOWLEDGMENTS

Publication is approved by all authors and by the responsible authorities where the work was carried out. Each author has participated sufficiently in any submission to take public responsibility for its content.

CONFLICT OF INTEREST

The authors have no conflicts of interest.

ETHICS STATEMENT

Written informed consent was obtained from all patients, and the study was approved by the ethics committee of the institution.

DATA AVAILABILITY STATEMENT

The data that support the findings of this study are available from the corresponding author upon reasonable request.

ORCID

Antonio Corvino https://orcid.org/0000-0002-6608-6252
Fabio Corvino https://orcid.org/0000-0002-2593-8148

REFERENCES

1. Barcaui EO, Carvalho AC, Piñeiro-Maceira J, et al. Study of the skin anatomy with high-frequency (22 MHz) ultrasonography and histological correlation. *Radiol Bras*. 2015;48:324-329.
2. Mandava A, Ravuri PR, Konathan R. High-resolution ultrasound imaging of cutaneous lesions. *Indian J Radiol Imaging*. 2013;23:269-277.
3. Wortsman X. Ultrasound in dermatology: why, how, and when? *Semin Ultrasound CT MRI*. 2013;34:177-195.
4. Crisan D, Lupsor M, Boca A, et al. Ultrasonographic assessment of skin structure according to age. *Indian J Dermatol Venereol Leprol*. 2012;78:519.
5. Daly SM, Leahy MJ. 'Go with the flow': a review of methods and advancements in blood flow imaging. *J Biophotonics*. 2013;6:217-255. https://doi.org/10.1002/jbio.201200071
6. Catalano O, Wortsman X. Dermatology ultrasound. Imaging technique, tips and tricks, high-resolution anatomy. *Ultrasound Q*. 2020;36:321-327.
7. Gaitini D. Introduction to color Doppler ultrasound of the skin. In: Wortsman X, ed. *Dermatologic Ultrasound with Clinical and Histologic Correlations*. Springer; 2013:3-14.
8. Wortsman X, Wortsman J, Carreno L, et al. In: Wortsman X, ed. *Sonographic Anatomy of the Skin, Appendages, and Adjacent Structures*. Springer; 2013:15-35.
9. Gniadecka M, Jemec GB. Quantitative evaluation of chronological ageing and photoageing in vivo: studies on skin echogenicity and thickness. *Br J Dermatol*. 1998;139:815-821.
10. Sandby-Møller J, Wulf HS. Ultrasonographic subepidermal low-echogenic band, dependence of age and body site. *Skin Res Technol*. 2004;10:57-63.
11. Seidenari S, Giusti G, Bertoni L, Magnoni C, Pellacani G. Thickness and echogenicity of the skin in children as assessed by 20-MHz ultrasound. *Dermatology*. 2000;201:218-222.
12. Bayramoglu Z, Kandemirli SG, Sarı ZNA, et al. Superb microvascular imaging in the evaluation of pediatric Graves disease and Hashimoto thyroiditis. *J Ultrasound Med*. 2020;39:901-909.
13. Chae EY, Yoon GY, Cha JH, Shin HJ, Choi WJ, Kim HH. Added value of the vascular index on superb microvascular imaging for the evaluation of breast masses: comparison with grayscale ultrasound. *J Ultrasound Med*. 2020;40:715-723. https://doi.org/10.1002/jum.15441
14. Park AY, Kwon M, Woo OH, et al. A prospective study on the value of ultrasound microflow assessment to distinguish malignant from benign solid breast masses: association between ultrasound parameters and histologic microvessel densities. *Korean J Radiol*. 2019;20:759-772.
15. Kanitakis J. Anatomy, histology and immunohistochemistry of normal human skin. *Eur J Dermatol*. 2002;12:390-399.
16. González Díaz CP. Characterization of dermatological lesions by ultrasound. *Rev Colomb Radiol*. 2014;25:4006-4014.
17. Gunin AG, Petrov VV, Golubtzova NN, Vasilieva OV, Kornilova NK. Age-related changes in angiogenesis in human dermis. *Exp Gerontol*. 2014;55:143-151.
18. Hara Y, Yamashita T, Kikuchi K, et al. Visualization of age-related vascular alterations in facial skin using optical coherence tomography-based angiography. *J Dermatol Sci*. 2018;90:96-98.
19. Morita TCAB, Trés GFS, Criado RFJ, Sotto MN, Criado PR. Update on vasculitis: an overview and dermatological clues for clinical and histopathological diagnosis—part I. *An Bras Dermatol*. 2020;95:355-371.
20. Braverman IM. The role of blood vessels and lymphatics in cutaneous inflammatory processes: an overview. *Br J Dermatol*. 1983;109(25):89-98.
21. Corvino A, Sandomenico F, Corvino F, et al. Utility of a gel stand-off pad in the detection of Doppler signal on focal nodular lesions of the

skin. *J Ultrasound*. 2020;23(1):45-53. https://doi.org/10.1007/s40477-019-00376-3
22. Hangiandreou NJ. AAPM/RSNA physics tutorial for residents. Topics in US: B-mode US: basic concepts and new technology. *Radiographics*. 2003;23:1019-1033.
23. Lawrence JP. Physics and instrumentation of ultrasound. *Crit Care Med*. 2007;35(8):S314-S322.
24. Jin W, Kim GY, Park SY, et al. The spectrum of vascularized superficial soft-tissue tumors on sonography with a histopathologic correlation: part 1, benign tumors. *AJR*. 2010;195:439-445.
25. Yoshimatsu H, Hayashi A, Yamamoto T, et al. Visualization of the "intradermal plexus" using ultrasonography in the dermis flap: a step beyond perforator flaps. *Plast Reconstr Surg Glob Open*. 2019;7:e2411.
26. Chami L, Lassau N, Chebil M, et al. Imaging of melanoma: usefulness of ultrasonography before and after contrast injection for diagnosis and early evaluation of treatment. *Clin Cosmet Investig Dermatol*. 2011;4:1-6.
27. Dubinsky TJ, Revels J, Wang S, et al. Comparison of superb microvascular imaging with color flow and power Doppler imaging of small hepatocellular carcinomas. *J Ultrasound Med*. 2018;37:2915-2924.
28. Jiang Z-Z, Huang Y-H, Shen H-L, Liu XT. Clinical applications of superb microvascular imaging in the liver, breast, thyroid, skeletal muscle, and carotid plaques. *J Ultrasound Med*. 2019;38:2811-2820.
29. Zhan J, Diao XH, Jin JM, Chen L, Chen Y. Superb microvascular imaging—a new vascular detecting ultrasonographic technique for avascular breast masses: a preliminary study. *Eur J Radiol*. 2016;85:915-921.
30. Govind D, Thomas KN, Hill BG, Van Rij AM. Microvenous reflux in the skin of limbs with superficial venous incompetence. *Ultrasound Med Biol*. 2018;44:756-761.
31. İslamoğlu ZGK, Uysal E. A preliminary study on ultrasound techniques applied to cicatricial alopecia. *Skin Res Technol*. 2019;25:810-814.
32. Jin W, Kim GY, Park SY, et al. The spectrum of vascularized superficial soft-tissue tumors on sonography with a histopathologic correlation: part 2, malignant tumors and their look-alikes. *AJR*. 2010;195:446-453.
33. Li H, Furst DE, Jin H, et al. High-frequency ultrasound of the skin in systemic sclerosis: an exploratory study to examine correlation with disease activity and to define the minimally detectable difference. *Arthritis Res Ther*. 2018;20:181.
34. Sen CK, Ghatak S, Gnyawali SC, Roy S, Gordillo GM. Cutaneous imaging technologies in acute burn and chronic wound care. *Plast Reconstr Surg*. 2016;138(3):119S-128S.

How to cite this article: Corvino A, Varelli C, Cocco G, Corvino F, Catalano O. Seeing the unseen with superb microvascular imaging: Ultrasound depiction of normal dermis vessels. *J Clin Ultrasound*. 2021;1-7. doi:10.1002/jcu.23068